STEM CELLS AND DEVELOPMENT
Volume 23, Number 16, 2014

DOI: 10.1089/scd.2013.0632

Netrin-1 Induces MMP-12-Dependent E-Cadherin Degradation Via the Distinct Activation of PKCα and FAK/Fyn in Promoting Mesenchymal Stem Cell Motility

Sei-Jung Lee,[1,2] Young Hyun Jung,[1,2] Sang Yub Oh,[1,2] Min Sik Yong,[1,2] Jung Min Ryu,[1,2] and Ho Jae Han[1,2]

Netrin-1 (Ntn-1) is a potent inducer of neuronal cell migration; however, its molecular mechanism that guides the migratory behavior of stem cells has not been characterized. In this study, we investigate the role of Ntn-1 in promoting the motility of human umbilical cord blood-derived mesenchymal stem cells (UCB-MSCs) and its related signaling pathways. Ntn-1 (50 ng/mL) significantly increased motility of UCB-MSCs, which was inhibited by blocking antibodies for deleted in colorectal cancer (DCC) and integrin (IN) α6β4. Ntn-1 in DCC stimulated protein kinase Cα (PKCα) activation, but not PKCε, PKCθ, and PKCζ, while Ntn-1 in INα6β4 induced the phosphorylation of focal adhesion kinase (FAK) and Fyn. Notably, Ntn-1 induced phosphorylation of extracellular signal-regulated kinases (ERK), c-Jun N-terminal kinases (JNK), and nuclear factor kappa-B (NF-κB), but they were concurrently downregulated by blocking the activities of PKCα, FAK, and Fyn. Ntn-1 uniquely increased the MMP-12 expression of all the matrix metalloproteinase (MMP) isoforms present in UCB-MSCs, though this was significantly blocked by an NF-κB inhibitor. Finally, Ntn-1 induced the MMP-12-dependent degradation of E-cadherin (E-cad), while Ntn-1 abrogated the interaction between E-cad and p120-catenin. In addition, Ntn-1 has the ability to stimulate cytoskeletal reorganization-related proteins, such as Cdc42, Rac1, Profilin-1, Cofilin-1, α-Actinin-4, and filamentous actin (F-actin) in UCB-MSCs. These results demonstrate that Ntn-1 induces MMP-12-dependent E-cad degradation via the distinct activation of PKCα and FAK/Fyn, which is necessary to govern the activation of ERK, JNK, and NF-κB in promoting motility of UCB-MSCs.

Introduction

Netrin-1 (Ntn-1), an evolutionary conserved family of laminin-related proteins, is a potent inducer of cell migration, cell–cell interactions, and cell-extracellular matrix adhesion during neuronal cell development [1,2]. Although the Ntn-1 signaling pathway in non-neuronal tissue has received little attention, many netrin receptors have been detected, not only in the nervous system [1,3], but also in a number of other tissues [2,4], where their functions remain largely unknown. We recently found that Ntn-1 protects the stem cells from hypoxia-induced mitochondrial apoptosis through the activation of Ntn-1 receptors, such as deleted in colorectal cancer (DCC) and integrin (IN) α6β4 [5]. In addition, Ntn-1 has been implicated in pancreatic development, where Ntn-1/integrin interactions induce the adhesion and migration of pancreatic progenitor cells [6]. However, the underlying cellular mechanisms and their receptor specificity characteristics involved in stem cell motility have yet to be studied.

Many studies have identified a number of important netrin signaling pathways and their effector molecules in neural development stages, such as focal adhesion kinase (FAK) [7], Src family kinases [7,8], small Rho-GTPases [9], and MAP-Kinases [10], which lead to the reorganization of the cytoskeleton. However, the coordination of signal transduction cascades downstream of different netrin receptors via effector molecules is still unclear. There are no previous reports related to the mechanism of the migration-promoting effects of tissue-affinitive Ntn-1 in stem cells. Thus, determining how netrin receptors and signal transduction proteins are systematically involved in regulating cell motility as an

[1]Department of Veterinary Physiology, Research Institute for Veterinary Science, College of Veterinary Medicine, Seoul National University, Seoul, Korea.
[2]BK21 PLUS Creative Veterinary Research Center, Seoul National University, Seoul, Korea.

ensemble remains a major challenge for current researchers. If this challenge can be overcome, netrin, netrin receptors, and their downstream signaling mechanisms could be promising targets for regulation of the stem cells functions.

Umbilical cord blood-derived mesenchymal stem cells (UCB-MSCs) are self-renewing multipotent progenitors with the potential to differentiate into multiple cell types, including osteoblasts, chondrocytes, and adipocytes [11]. UCB-MSCs are easy to isolate and have low immunogenicity, multidifferentiation potentials, and remain free of any ethical controversy [11–13]. Due to the migration ability of MSCs via circulation to sites of tissue damage, the therapeutic value of MSCs has been evaluated in many clinical applications [14–16]. In addition, many studies have focused on the development of new molecules that regulate MSC migration in wound healing, damage repair, and regeneration [17–20]. In this study, we investigate the role of Ntn-1 in promoting the motility of UCB-MSCs and its related signaling pathways.

Materials and Methods

Materials

Human UCB-MSCs were kindly provided by Medipost Co. (Seoul, Korea), which was isolated and expanded as reported previously [11]. These cells have been characterized to express CD105 (99.6%) and CD73 (96.3%), but not CD34 (0.1%), CD45 (0.2%), and CD14 (0.1%). They were positive for HLA-AB but generally not for HLA-DR [11]. The human UCB-derived MSCs differentiated into various cell types such as osteoblasts, chondrocytes, and adipocytes upon in vitro induction with the appropriate osteogenic, chondrogenic, and adipogenic differentiation stimuli [11]. Human adipose-derived mesenchymal stem cells (AD-MSCs) were kindly provided by Prof. Kyung-Sun Kang (Seoul National University, Korea). In this study, all the experiments were carried out with cells of seven passages. Fetal bovine serum (FBS) was purchased from BioWhittaker, Inc. (Walkersville, MO). Phospho-ERK1/2, extracellular signal-regulated kinases (ERK), phospho-JNK/SAPK, JNK/SAPK, phospho-p38 MAPK, and p38 MAPK antibodies were obtained from the R&D System (Minneapolis, MN). A23187, bisindolylmaleimide I, PD98059, SP600125, staurosporine, MMP408, and mitomycin C were obtained from Sigma Chemical Company (St. Louis, MO). SN 50 was purchased from Calbiochem (La Jolla, CA). Bay11-7082 was purchased from Biomol International (Plymouth Meeting, PA). α-Actinin-1, α-Actinin-4, β-actin, Cdc42, E-cadhrin (E-cad), phospho-Cofilin-1, Cofilin-1, phospho-Fyn, Fyn, phospo-FAK, FAK, matrix metalloproteinase (MMP)-12, phospho-NF-κB (p65), nuclear factor kappa-B (NF-κB), protein kinase C (PKC), PKCα, PKCε, PKCθ, and PKCζ, p120-catenin, Profilin-1, Rac1, and RhoA antibodies were purchased from Santa Cruz Biotechnology (Santa Cruz, CA). Filamentous actin (F-actin) and phospho-PKC antibodies were purchased from Cell Signaling (Beverly, MA). Horseradish peroxidase (HRP)-conjugated goat anti-rabbit and goat anti-mouse IgG were purchased from Jackson Immunoresearch (West Grove, PA). All other reagents were of the highest purity commercially available and were used as received.

Culture of human UCB-MSCs and AD-MSCs

Human UCB-MSCs and AD-MSCs were cultured without a feeder layer in the α-minimum essential medium (α-MEM; Thermo, Waltham, MA) and keratinocyte-serum-free medium, respectively. The cells were grown in 1% penicillin and streptomycin, and 10% FBS. For each experiment, cells were grown in wells of 6- and 12-well plates, and in 35, 60, or 100-mm diameter culture dishes in an incubator maintained at 37°C with 5% CO_2. The medium was replaced with serum-free α-MEM at least 24 h before experiments. Following incubation, the cells were washed twice with phosphate-buffered saline (PBS) and then maintained in a serum-free α-MEM including all supplements and indicated agents.

Wound-healing migration assay

Human UCB-MSCs were seeded at 4×10^4 cells on low 35-mm dishes with both silicone reservoirs, which are separated by a 500-μm thick wall (Ibidi, Martinsried, Germany) [21] and incubated until the cell reached around 100% confluence in serum-containing medium. After serum starvation for 24 h, the silicone reservoirs were removed with sterile forceps to create a wound field. The cells were incubated for an additional 24 h with Ntn-1 (50 ng/mL) and visualized with an Olympus FluoView™ 300 confocal microscope with 100× objective.

Oirs™ cell migration assay

Human UCB-MSCs were seeded at 3×10^2 cells/100 μL in Oirs well (Platypus Technologies, Fitchburg, WI) and incubated for 24 h to permit cell adhesion. Inserts were carefully removed when the cell reached around 70% confluence, and the wells were gently washed with culture medium. Cells were then incubated with Ntn-1 (50 ng/mL) and serum-free medium. Cell motility was microscopically observed after 24 h. Cell populations in endpoint assays were stained with 5 μM calcein AM for 30 min. Migrated cells were quantified through measurement of fluorescence signals by using a microplate reader at excitation and emission wavelengths of 485 and 515 nm, respectively [22].

Transwell migration assay

In vitro transwell migration assay was performed in transwell permeable support with 8.0-μm pore size membrane (Corning Incorporated Life Sciences, Lowell, MA) according to the manufacturer's instruction. UCB-MSCs suspensions (5×10^4 cells/mL) were placed into the upper chamber in 0.2 mL of serum-free medium. The lower compartment was filled with 0.6 mL serum-free medium containing 50 ng/mL Ntn-1. After incubation for 24 h, cells that had migrated to the lower surface of the filters were fixed in acetone for 5 min at room temperature and visualized with hematoxylin and eosin staining method. The number of migrated cells at the lower side per total input (initial UCB-MSCs suspensions) was calculated and converted the number to a percentage by multiplying by 100.

RNA isolation and real-time polymerase chain reaction

Total RNA was extracted from human UCB-MSCs using the RNeasy Plus Mini Kit (Quiagen, Valencia, CA). To

synthesize cDNA, reverse transcription (RT) was carried out with 3 μg of RNA using a Maxime RT premix kit (iNtRON Biotechnology, Sungnam, Korea). The real-time quantification of *MMP* family was performed using a Rotor-Gene 6000 real-time thermal cycling system (Corbett Research, New South Wales, Australia) with a QuantiMix SYBR Kit (PhileKorea Technology, Daejeon, Korea), 200 ng cDNA, and primers, The primers used are described in Supplementary Table S1 (Supplementary Data are available online at www.liebertpub.com/scd). Data were collected during the extension step and analyzed using the manufacturer's software. To verify the specificity and identity of polymerase chain reaction (PCR) products, the amplification cycles were followed by a high resolution melting cycle from 65°C to 99°C at a rate of 0.1°C/2 s. When the melting temperature was reached, double-stranded DNA was denatured and the SYBR was released, which caused a dramatic decrease in fluorescence intensity. The rate of this change was determined by plotting the derivative of the fluorescence relative to the temperature (dF/dT) versus temperature by data analysis software of the real-time PCR instrument. The temperature at which a peak occurred on the plot corresponded to the temperature of the DNA duplex. β-Actin was used as an endogenous control.

Immunofluorescence microscopy

Cells were plated onto coverslips (Thickness: No 1, Size: 18 mm) (Thermo Fisher Scientific, Rockford, IL) and fixed with 4% paraformaldehyde in PBS, permeabilized for 10 min with 0.1% (vol/vol) Triton X-100, and washed twice for 10 min each with PBS. Cells, preincubated with 10% bovine serum albumin (BSA; Sigma-Aldrich) in PBS for 20 min to decrease nonspecific antibody binding, were incubated for 60 min with a 1:100 dilution of primary antibody in a solution containing 1% (v/v) BSA in PBS, and washed thrice for 10 min each with PBS. Cells were then incubated with 1% (v/v) BSA for 5 min, incubated for 60 min with anti-rabbit, -mouse, and -goat IgG-FITC (green) antibody, counterstained with propidium iodide (PI) in PBS containing 1% (v/v) BSA, and washed thrice for 10 min each with PBS. Samples were mounted on slides and visualized with an Olympus FluoView 300 confocal microscope with 400× objective. The expressions of p-FAK, p-Fyn, MMP-12. p-Cofilin-1, Profilin-1, and α-Actinin-4 in immunofluorescence image were quantified by using Image J software (NIH, Bethesda, MD), which measures the stained area per microscopic filed with consistent threshold. On the other hand, the cell numbers showing the membrane translocation of PKCα, Cdc42, and Rac1, and the nuclear translocation of phospho-NF-κB were directly counted per random microscopic filed and converted the numbers to a percentage by multiplying by 100. Ten random fields per coverslip were counted.

Phalloidin staining

Cells were washed with warm PBS, fixed with 3.7% formaldehyde for 10 min, and permeabilized with 0.5% Triton X-100 in PBS for 10 min before incubating with Alexa Fluor 488-conjugated to phalloidin (Invitrogen Co., Carlsbad, CA) for 30 min. Cells were then washed five times (thrice with PBS containing 0.02% BSA followed by twice with PBS). Samples were mounted on slides and visualized with an Olympus FluoView 300 confocal microscope (Tokyo, Japan) with 400× objective.

Small interfering RNA transfection

Cells were grown until 75% of the surface of the plate and transfected for 24 h with small interfering RNAs (siRNAs) specific for *FAK* (200 pM; GenePharma, Shanghai, China), *Fyn* (200 pM), *MMP-12* (200 pM), or a nontargeting siRNA as a negative control (200 pM) with Hyperfectamine (QIAGEN, Valencia, CA) according to the manufacturer's instructions. The sequences used are described in Supplementary Table S2 and determined siRNA efficacy for FAK, Fyn, and MMP-12, respectively (Supplementary Fig. S1).

Western blot analysis

Cells were harvested, washed twice with PBS, and lysed with buffer [20 mM Tris (pH 7.5), 1 mM EDTA, 1 mM EGTA, 1% Triton X-100, 1 mg/mL aprotinin, and 1 mM phenylmethylsulfonylfluoride (PMSF)] for 30 min on ice. The lysates were then cleared by centrifugation (22,250 *g* at 4°C for 30 min). Protein concentration was determined by the Bradford method [23]. Equal amounts of protein (20 μg) were resolved by 10% sodium dodecyl sulfate polyacrylamide gel electrophoresis (SDS-PAGE) and transferred to polyvinylidene fluoride (PVDF) membranes. The membranes were washed with TBST solution [10 mM Tris-HCl (pH 7.6), 150 mM NaCl, and 0.05% Tween-20], blocked with 5% skim milk for 1 h, and incubated with appropriate primary antibody at 4°C for overnight. The membrane was then washed and detected with a HRP-conjugated secondary antibody. The bands were visualized by enhanced chemiluminescence (Amersham Pharmacia Biotech, Inc., Buckinghamshire, United Kingdom).

Trichloroethanoic acid precipitation

Filtered culture supernatants were mixed with trichloroethanoic acid (TCA) to a final concentration of 30% (w/v) and were incubated on ice for 30 min or stirred overnight at 4°C. Samples were centrifuged at 10,000 *g* for 20 min. Pellets were washed with ice-cold 96% ethanol (v/v) and acetone, and were air-dried.

Measurement of calcium influx

Changes in intracellular calcium concentrations were monitored using Fluo-3-AM that had initially been dissolved in dimethylsulfoxide (DMSO). Cells in 35 mm-diameter culture dishes were rinsed with a bath solution [140 mM NaCl, 5 mM KCl, 1 mM $CaCl_2$, 0.5 mM $MgCl_2$, 10 mM glucose, 5.5 mM HEPES (pH 7.4)] and were then incubated in a bath solution containing 3 μM Fluo-3-AM for 40 min, rinsed, mounted on a perfusion chamber, and scanned at 1 s intervals using Olympus FluoView 300 confocal microscope with 300× objective. The fluorescence was produced by excitation at 488 nm and the emitted light was observed at 515 nm. All analyses of calcium influx were processed in a single cell, and the results are expressed as the fluorescent intensity (F/F_0%, arbitrary unit, where F is fluorescence captured at a particular time and F_0 is initial fluorescence image captured).

Immunoprecipitation

Interaction of p120-catenin with E-cad was analyzed by immunoprecipitation and western blotting. Cells were lysed with lysis buffer (1% Triton X-100 in 50 mM Tris–HCl pH 7.4 containing 150 mM NaCl, 5 mM EDTA, 2 mM Na_3VO_4, 2.5 mM Na_4PO_7, 100 mM NaF, 200 nM microcystin lysine–arginine, and protease inhibitors). Cell lysates (400 mg) were mixed with 10 mg of mouse anti-p120-catenin. The samples were incubated for 4 h, mixed with Protein A/G PLUS-agarose immunoprecipitation reagent (Pierce, Rockford, IL), and then incubated for an additional 12 h. The beads were washed four times, and the bound proteins were released from the beads by boiling in SDS-PAGE sample buffer for 5 min. Samples were analyzed by western blotting with rabbit anti-E-cad antibody.

Affinity precipitation of cellular GTP-Cdc42, -Rac1, and -RhoA

Activation of Cdc42, Rac1, and RhoA activities were determined by using an affinity precipitation assay kits (EMD Millipore, Billerica, MA) according to the manufacturer's instructions. Cells starved for 24 h were stimulated with Ntn-1 and lysed for 5 min in ice-cold cell lysis buffer. Four hundred micrograms of lysates were incubated for 1 h with agarose beads coupled with the Cdc42/Rac-binding domain (GST-PAK-PBD) or with Rho-binding domain of rhotekin (GST-Rhotekin-RBD), and the bound Cdc42, Rac1, and RhoA proteins were eluted with 2× laemmli sample buffer and subjected to western blot using anti-Cdc42, anti-Rac1, and anti-RhoA antibodies, respectively.

Statistical analysis

Results are expressed as mean ± standard errors. All experiments were analyzed by ANOVA, followed in some cases by a comparison of treatment means with the control using the Bonferroni-Dunn test. Differences were considered statistically significant at $P < 0.05$.

Results

Effects of Ntn-1 on human UCB-MSC motility

To examine the role of Ntn-1 in motility of UCB-MSCs, cells were exposed to various concentrations (0.01–100 ng/mL) of Ntn-1 for 24 h. As shown in Fig. 1A, Ntn-1 significantly induced cell motility of UCB-MSCs from 0.1 to 100 ng/mL in a dose-dependent manner. In addition, an increase in cell motility was observed after 8 h incubation with 50 ng/mL Ntn-1 (Fig. 1B). We further visualized the ability of 50 ng/mL Ntn-1 to induce cell motility for 24 h by staining the cells with calcein AM in Oris cell migration assay. In contrast to the control, Ntn-1 significantly induced translocation of cell bodies into the denuded area for wound healing (167% increase compared to the control; $P < 0.05$) (Fig. 1C). The effect of Ntn-1 in cell motility was further accessed by transwell migration assay. As shown in Supplementary Fig. S2A, we found Ntn-1 significantly increased the cell numbers that had migrated to the lower surface of the membrane. We further quantified the absolute migration percentage based on the results of transwell migration assay (Supplementary Fig. S2B). The control cells that had migrated to the lower surface of the filters were 1.71% of total input. In contrast, 4.18% cells were moved to the lower surface in response to Ntn-1 treatment. In addition, Ntn-1 (50 ng/mL) significantly induced the motility of human AD-MSCs (Supplementary Fig. S3). This result suggests that the functional role of Ntn-1 to induce the motility is reproducible in other types of MSCs.

On the other hand, the cells were treated with Ntn-1 either in the presence or absence of blocking antibodies for DCC and INα6β4 to determine the specificity of Ntn-1 in receptor-binding activity. The cell migration-promoting activity of Ntn-1 was attenuated by DCC or INα6β4 antibodies (Fig. 1D). The effect of Ntn-1 in cell motility was further visualized by staining the filamentous (F)-actin structure with Alexa Fluor® 488-conjugated phalloidin (Fig. 1E). Additionally, mitomycin C (1 μg/mL), a cell cycle arresting compound, did not inhibit Ntn-1-induced cell motility (Fig. 1F). On the other hand, we further investigated whether Ntn-1 regulates FBS-induced migration of UCB-MSCs. Supplementary Fig. S4A showed that 1% FBS induced the motility at 24 h. In Ntn-1-treated cells, the FBS was sufficient to speed up the cell migration within 16 h. These results indicate that Ntn-1 has enhancing effect on FBS-induced migration. However, the cell migration-promoting activity of FBS was not attenuated by DCC or INα6β4 antibodies (Supplementary Fig. S4B). Thus, these results suggest that the effect of Ntn-1 in promoting cell motility is an independent process of FBS and is unique Ntn-1 receptor signaling pathway.

Effect of Ntn-1 on activation of PKC, FAK, and Fyn

Since Ntn-1 binding to DCC regulates phospholipase C (PLC) signaling [24], we further assessed whether Ntn-1 induces phosphorylation and translocation of PKC as an important downstream intermediate of PLC in human UCB-MSCs. Ntn-1 increased PKC phosphorylation from 15 to 90 min (Fig. 2A). In addition, translocation of PKCα, but not PKCε, PKCθ, and PKCζ from the cytosol to the membrane compartment was observed after cells were treated with 50 ng/mL Ntn-1 for 60 min (Fig. 2B). Membrane translocation of PKCα was further confirmed by immunofluorescence staining in Ntn-1-treated UCB-MSCs (Fig. 2C). However, Ntn-1 did not stimulated calcium influx, which was enhanced by A23187, as a positive control (Fig. 2D). The effect of Ntn-1 on phosphorylation of FAK and Fyn, which were believed to be essential factors in netrin signaling pathways, was further examined. Ntn-1 (50 ng/mL) significantly induced the phosphorylation of FAK and Fyn at 60 min (Fig. 2E). Increased staining of p-FAK and p-Fyn were observed after cells were treated with 50 ng/mL Ntn-1 for 60 min (Fig. 2F). Interestingly, pretreatment with DCC-blocking antibody significantly blocked Ntn-1-induced phosphorylation of PKC, but no effect was observed on FAK and Fyn phosphorylation (Fig. 2G). In contrast, the INα6β4-blocking antibody inhibited Ntn-1-induced phosphorylation of FAK and Fyn but did not affect PKC phosphorylation (Fig. 2G).

Effect of Ntn-1 on activation of MAPK and NF-κB

We then determined how Ntn-1 links to the activation of MAPKs that are interesting candidates for the downstream

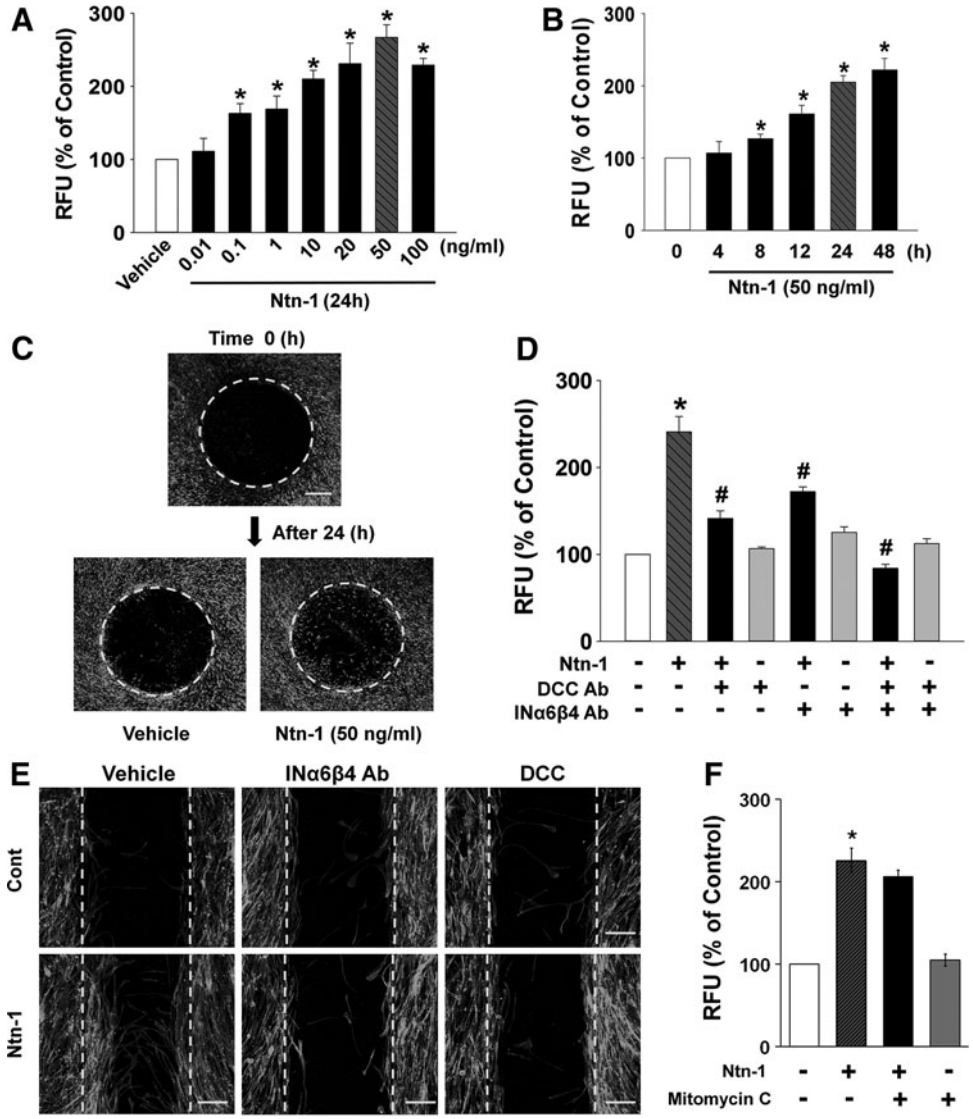

FIG. 1. Effects of Ntn-1 on human UCB-MSC migration. **(A)** Dose response of Ntn-1 in Oris™ cell migration assay. Cells were treated with different doses of Ntn-1 (0.01–100 ng/mL) for 24 h. Fluorescence in the analytical zone was quantified with a plate reader. Data represent mean ± SE of five independent experiments with triplicate dishes. $^{*}P < 0.05$ versus vehicle. **(B)** Time response of Ntn-1 in Oris cell migration assay. Cells were treated with 50 ng/mL Ntn-1 for various times (0–48 h). $^{*}P < 0.05$ versus 0 h. **(C)** Cells treated with 50 ng/mL Ntn-1 for 24 h were visualized by calcein AM staining using Oris cell migration assay. $n = 5$. Scale bars represent 200 μm (magnification, × 40). **(D)** Cells were pretreated with DCC blocking antibody (2.5 μL/mL) or combination of INα6 and INβ4-blocking antibodies (2.5 μL/mL) for 30 min prior to Ntn-1 exposure for 24 h. Oris cell migration assay was performed and quantified the value of fluorescence. Data represent mean ± SE of five independent experiments with triplicate dishes. $^{*}P < 0.01$ versus vehicle. $^{\#}P < 0.01$ versus Ntn-1 alone. **(E)** Wound-healing assay was performed and stained with phalloidin-AlexaFluor 488 to identify the migrating cells. $n = 5$. Scale bars represent 100 μm (magnification, × 100). **(F)** Effect of mitomycin C in Ntn-1-induced cell migration. Cells were pretreated with 1 μg/mL mitomycin C for 30 min prior to 50 ng/mL Ntn-1 exposure for 24 h. Oris cell migration assay was performed and quantified the value of fluorescence. Data represent mean ± SE of four independent experiments with triplicate dishes. $^{*}P < 0.01$ versus vehicle. DCC, deleted in colorectal cancer; IN, integrin; Ntn-1, Netrin-1; RFU, relative fluorescence units; SE, standard errors; UCB-MSCs, umbilical cord blood-derived mesenchymal stem cells.

mediators of PKC, FAK, and Fyn in both cell migration and axon growth [1]. Phosphorylation of ERK and c-Jun N-terminal kinases (JNK) increased for 60–120 min in response to Ntn-1 (Fig. 3A), but did not affect p38 MAPK phosphorylation, and its effect was inhibited by PKC inhibitors, bisindolylmaleimide I and staurosporine (Fig. 3B) in addition to gene silencing of *FAK* and *Fyn* (Fig. 3C). These data provide the important evidence that ERK/JNK phosphorylation is concurrently regulated by activation of both PKC and FAK/Fyn that are required for regulation of UCB-MSC motility induced by Ntn-1. We further examined the role of Ntn-1 in activation of NF-κB, which is a direct transcriptional target for Ntn-1 receptor signaling pathway [25]. As shown in Fig. 3D, NF-κB phosphorylation

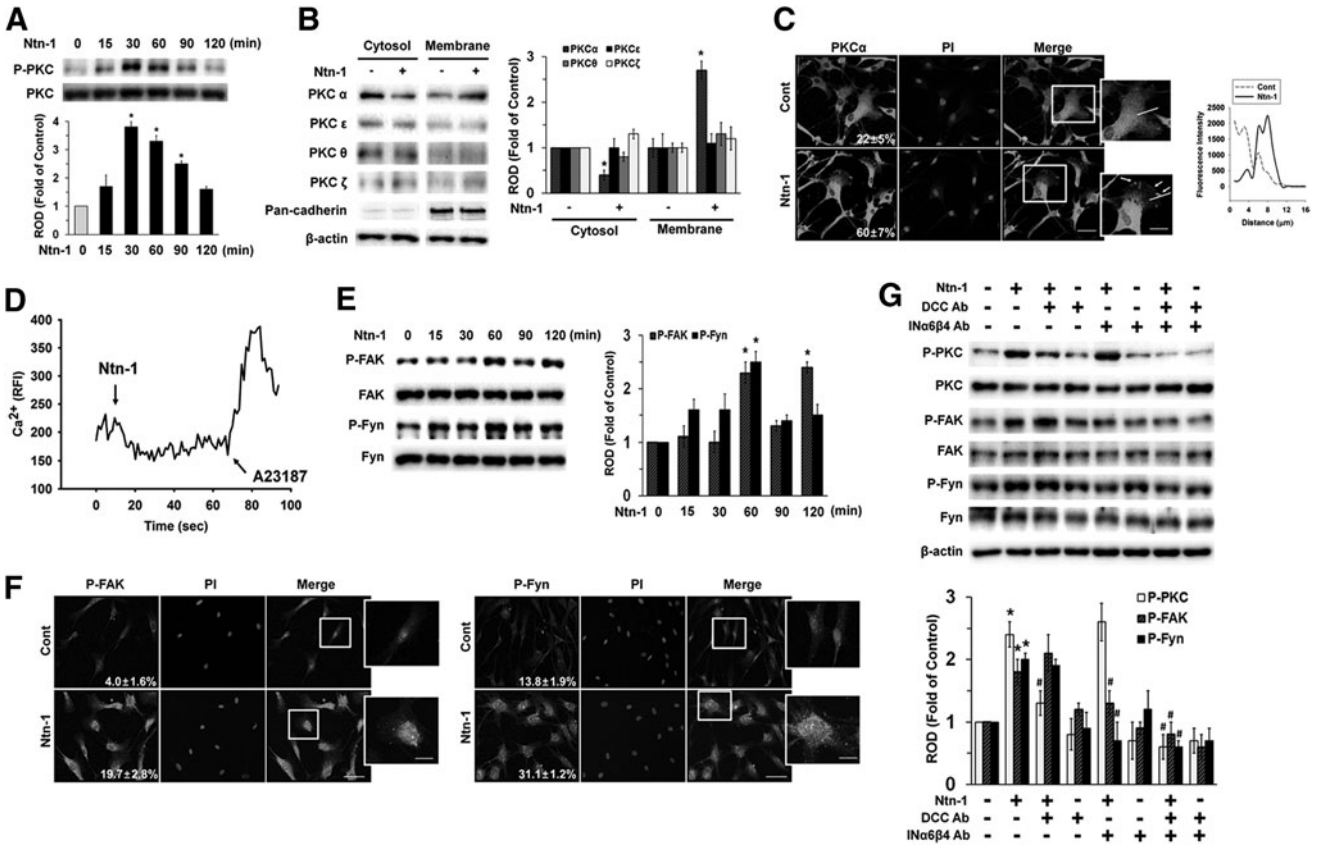

FIG. 2. Effect of Ntn-1 on activation of PKC, FAK, and Fyn. **(A)** The cells were incubated in the presence of Ntn-1 (50 ng/mL) for various times (0–120 min) and then harvested. Total protein was extracted and blotted with phospho- and total-PKC antibodies. Changes in PKC phosphorylation by Ntn-1 relative to total PKC were determined by densitometric analysis of western blots. Error bars represent mean ± SE from three independent experiments involving triplicates. $^{*}P < 0.05$ versus 0 h. **(B)** The cells were stimulated with Ntn-1 (50 ng/mL) for 60 min, and extracted proteins for cytosolic and membrane. Western blot analysis was performed to detect PKC translocation of PKC isoforms. Changes in membrane translocation of PKC isoforms by Ntn-1 relative to β-actin were determined by densitometric analysis of western blots. The pan-cadherin was used as a plasma membrane control. Error bars represent mean ± SE from three independent experiments involving triplicates. $^{*}P < 0.01$ versus vehicle. **(C)** The cells were treated with Ntn-1 (50 ng/mL) for 60 min. PKCα was detected by immunostaining with PKCα antibody. *Arrows* indicate membrane translocation of PKCα. The cell numbers showing membrane translocalization of PKCα per microscopic filed were directly counted and converted to a percentage by multiplying by 100. Ten random fields per coverslip were counted. The quantification data of immunofluorescence images were presented as mean ± SE of three independent experiments. The profiles in the *right panel* show the fluorescence intensity of PKCα from line (*solid line*) scans in the merged images, which were analyzed by FluoView™ 300 software (Olympus; Tokyo, Japan). Scale bars represent 100 μm (magnification, ×400). PI was used for nuclear counterstaining. **(D)** The cells were loaded with 2 μM Fluo-3/AM in serum-free medium for 40 min and treated with Ntn-1 (50 ng/mL). Cells were then treated with A23187 (10 μM, Ca^{2+} ionophore) as a positive control. Changes in $[Ca^{2+}]_i$ were monitored by confocal microscopy, and data are expressed as relative fluorescence intensity (F/F0%, arbitrary unit). **(E)** The cells were incubated in the presence of Ntn-1 (50 ng/mL) for various times (0–120 min) and then harvested. Total protein was extracted and blotted with phospho- and total-FAK and Fyn antibodies. Error bars represent mean ± SE from three independent experiments involving triplicates. $^{*}P < 0.05$ versus 0 h **(F)** The cells were treated with Ntn-1 (50 ng/mL) for 60 min. The phosphorylations of FAK (*left panel*) and Fyn (*right panel*) were detected by immunostaining with p-FAK and p-Fyn antibodies, and quantified by using Image J program, which measures the stained area per microscopic filed with consistent threshold. The quantification data of immunofluorescence images were presented as mean ± SE of three independent experiment. Scale bars represent 100 μm (magnification, ×400). PI was used for nuclear counterstaining. **(G)** Cells were pretreated with DCC-blocking antibody (2.5 μL/mL) or combination of INα6- and INβ4-blocking antibodies (2.5 μL/mL) for 30 min prior to Ntn-1 exposure for 60 min; phospho and total form of PKC, FAK, and Fyn were detected by western blot. Changes in phospho-PKC, phospho-FAK, and phospho-Fyn by Ntn-1 relative to PKC, FAK, and Fyn were determined by densitometric analysis of western blots. Error bars represent mean ± SE from three independent experiments involving triplicates. $^{*}P < 0.05$ versus vehicle. $^{\#}P < 0.05$ versus Ntn-1 alone. FAK, focal adhesion kinase; PI, propidium iodide; PKC, protein kinase C.

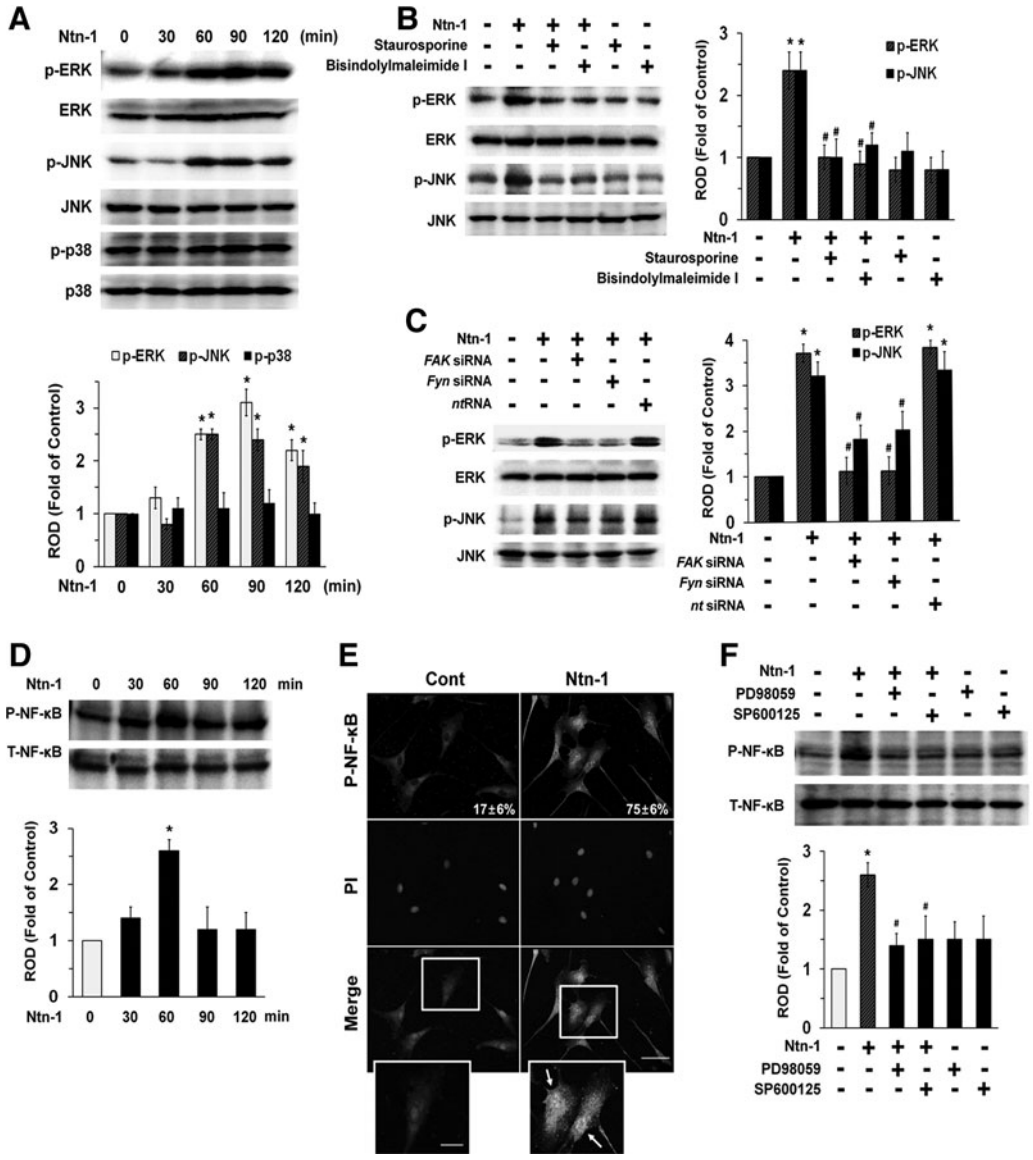

FIG. 3. Effect of Ntn-1 on activation of mitogen-activated protein kinase (MAPK) and nuclear factor kappa-B (NF-κB). **(A)** The cells were incubated in the presence of Ntn-1 (50 ng/mL) for various times (0–120 min) and then harvested. Total protein was extracted and blotted with phospho-ERK (P-ERK), phospho-JNK (P-JNK), phospho-p38 (P-p38), total-ERK (T-ERK), total-JNK (T-JNK), and total-p38 (T-p38) antibodies. Error bars represent mean ± SE from four independent experiments involving triplicates. $^{*}P < 0.05$ versus 0 h. **(B)** Cells were pretreated with PKC inhibitors bisindolylmaleimide I (10 μM) and staurosporine (10 μM) for 30 min prior to Ntn-1 (50 ng/mL) exposure for 60 min. Total protein was extracted and blotted with P-ERK, P-JNK, T-ERK, and T-JNK antibodies. **(C)** Cells were transfected for 24 h with specific siRNA for *FAK* and *Fyn* (200 pM) using Hyperfectamine before Ntn-1 (50 ng/mL) exposure for 60 min. Nontargeting (*nt*) control siRNA was used as a negative control (200 pM). **(D)** The cells were incubated in the presence of Ntn-1 (50 ng/mL) for various times (0–120 min) and then the phosphorylation of NF-κB was determined by western blot with phospho-NF-κB (P-NF-κB) and total-NF-κB (T-NF-κB) antibodies. **(E)** The cells were treated with Ntn-1 (50 ng/mL) for 60 min. P-NF-κB was detected by immunostaining with P-NF-κB antibody. *Arrows* indicate nuclear translocation of P-NF-κB. The cell numbers showing nuclear translocalization of P-NF-κB per microscopic filed were directly counted and converted to a percentage by multiplying by 100. Ten random fields per coverslip were counted. The quantification data of immunofluorescence images were presented as mean ± SE of three independent experiments. Scale bars represent 100 μm (magnification, ×400). PI was used for nuclear counterstaining. **(F)** Cells were pretreated with ERK inhibitor, PD98059 (10 μM) and JNK inhibitor, SP600125 (10 μM) for 30 min prior to Ntn-1 (50 ng/mL) exposure for 60 min. The phosphorylation of NF-κB was determined by western blot with P-NF-κB and T-NF-κB antibodies. **(B–D, F)** Each example shown is representative of four independent experiments. Changes in P-ERK, P-JNK, P-38, and P-NF-κB by Ntn-1 relative to T-ERK, T-JNK, T-p38, and T-NF-κB were determined by densitometric analysis of western blots. Error bars represent mean ± SE from four independent experiments involving triplicates. $^{*}P < 0.01$ versus vehicle. $^{\#}P < 0.01$ versus Ntn-1 alone. JNK, c-Jun N-terminal kinases; ERK, extracellular signal-regulated kinases; NF-κB, nuclear factor kappa-B; ROD, relative optical density; siRNA, small interfering RNA.

increased at 60 min after Ntn-1 treatment. The increased accumulation of NF-κB phosphorylation in the nucleus was further confirmed by immunofluorescence staining and counter-labeling with PI (Fig. 3E). In addition, pretreatment with the ERK inhibitor, PD98059 and JNK inhibitor, SP600125 significantly blocked Ntn-1-induced phosphorylation of NF-κB (Fig. 3F).

Effect of Ntn-1 on the degradation of E-cad via MMP-12 and on cytoskeletal reorganization

Having demonstrated the necessity of NF-κB in regulation of cell motility by Ntn-1, we wondered how activated NF-κB actually coordinates with cell–cell adhesion molecule or extracellular matrix. Although several NF-κB targets are likely to be involved in this process, one way it can do is to regulate the expression of the MMPs, which are essential enzymes to digest basement membrane in tissue remodeling and migration. As shown in Fig. 4A, we found Ntn-1 selectively augmented the *MMP-12* mRNA expression level among various kinds of MMPs mRNA amplicons, such as *MMP-1*, *-2*, *-11*, *-12*, *-14*, *-16*, *-17*, and *-19*, present in UCB-MSCs. However, *MMP-3*, *-7*, *-8*, *-9*, *-10*, *-13*, *-15*, and *-26* were not expressed in UCB-MSCs (data not shown). Interestingly, Ntn-1 participated in increased protein expression of MMP-12 in both lysates and medium, which was precipitated by TCA (Fig. 4B). The increased MMP-12 expression induced by Ntn-1 treatment was further confirmed by immunofluorescence staining (Fig. 4C). We then asked whether MMP-12 expression is regulated by activation of NF-κB. Pretreatment of NF-κB inhibitor, Bay 11-7082, blocked Ntn-1-induced MMP-12 expression in both lysates and medium (Fig. 4D). To ensure the functional role of MMP-12, we further determined whether Ntn-1 regulates degradation of E-cadherin (E-cad) as a major protein in cell adherens junctions [26]. As shown in Fig. 4E, Ntn-1 decreased E-cad expression, but it did not regulate the expression of p120-catenin, which is another adherens junctional protein to stabilize the cadherin–catenin complex [27]. However, Ntn-1 significantly abrogated the interaction between p120-catenin and E-cad (Fig. 4F) and Ntn-1-induced E-cad degradation was inhibited by the *MMP-12* siRNA (Fig. 4G), suggesting that MMP-12 plays a critical role in degradation of E-cad, thereby destabilizing adherens junctions to enhance the cell migration in response to Ntn-1.

To examine the potential role of Ntn-1 in promoting cell motility beyond the reach of regulation of MMP-12-dependent E-cad degradation, we further determined whether Ntn-1 regulates cytoskeletal reorganization-related proteins that are responsible for cell motility. Affinity precipitation for small Rho GTPases revealed that Cdc42 and Rac1 activities, but not RhoA were increased by treatment with 50 ng/mL Ntn-1 (Fig. 4H). In addition, an increase in F-actin expression was observed after 12 h incubation with 50 ng/mL Ntn-1 (Fig. 4I). The effect of Ntn-1 on Profilin-1, Cofilin-1, and α-Actinins levels, which is believed to be essential in the dynamic regulation of F-actin was further examined. Treatments with Ntn-1 increased Cofilin-1 phosphorylation and expression of Profilin-1 and α-Actinin-4, but not α-Actinin-1, respectively (Fig. 4J). The increased level of the cytoskeletal reorganization-related proteins induced by Ntn-1 treatment was further confirmed by immunofluorescence staining. Ntn-1 significantly induced the membrane translocation of Cdc42 and Rac1 (Supplementary Fig. S5A, B) and the phosphorylation of Cofilin-1 (Supplementary Fig. S5C), and enhanced the expression of Profilin-1 and α-Actinin-4 in UCB-MSCs (Supplementary Fig. S5D, E). In addition, we further examined whether there are changes in actin filament organization during directional cell migration (Supplementary Fig. S6). In quiescent cells before Ntn-1 stimulation, the actin cytoskeleton formed thin actin bundles with week immunofluorescence staining for phalloidin, which binds to actin filaments. However, Ntn-1 significantly induced translocation of cell bodies into the denuded area for wound healing, where the cells were densely packed with thick stress fibers having well organized actin cytoskeletal network. This result indicates Ntn-1 is able to stimulate morphological transformation/cytoskeletal reorganization by increasing F-actin expression to promote cell migration.

To confirm that the effect of Ntn-1 in promoting human UCB-MSCs motility is mediated through its related signaling molecules proved by our study, we further determined the effect of siRNAs and inhibitors on activation of Ntn-1 signaling pathway in UCB-MSCs motility. We pretreated cells with staurosporine, bisindolylmaleimide I, *FAK siRNA*, *Fyn siRNA*, and *nt siRNA* to confirm PKC and FAK/Fyn involvement (Fig. 5A), PD98059, SP600125, Bay 11-7082, and SN 50 to show ERK/JNK/NF-κB involvement (Fig. 5B), and MMP408, *MMP-12* siRNA, and *nt*RNA to prove MMP-12 involvement (Fig. 5C) prior to Ntn-1 exposure for 24 h. As expected, the Ntn-1-induced increase in cell motility was significantly abrogated by all blockers for PKC, FAK/Fyn, ERK, JNK, NF-κB, and MMP-12, respectively.

Discussion

In this study, we introduce two novel findings regarding the physiological role of Ntn-1 in stem cells. First, we found that Ntn-1 has ability to stimulate MMP-12-mediated E-cad degradation in promoting the migration of UCB-MSCs. Second, our biochemical and functional studies revealed that Ntn-1 triggers the distinct activation of DCC/PKCα and INα6β4/Fyn/FAK, which are responsible for the induction of ERK/JNK/NF-κB pathway, suggesting potentially novel means of promoting recovery from cellular injury and achieving improvements in tissue regeneration. Thus, our findings suggest that Ntn-1 is a good candidate for cell transplantation as supplemental agent that induces stem cell motility. This result is supported by a previous report by the authors, which revealed that Ntn-1 is critical for the stem cell survival and migration [5,28]. We believe that these broad effects of Ntn-1 are in part due to the presence of multiple Ntn-1 receptors in different types of cells and that it may vary depending on the cellular concept. We recently have reported that UCB-MSCs express both DCC and INα6β4, which are the key functional receptors of Ntn-1 for stem cell survival [5]. To ascertain that DCC and INα6β4 are primary Ntn-1 receptors regulating UCB-MSCs motility, we employed mechanically wounded monolayers model to achieve directionally persistent migration by forming and stabilizing actin-rich protrusions or lamellipodia [29]. We found that both DCC and INα6β4 are required for Ntn-1-induced cell migration, suggesting that Ntn-1 may have unique receptor signaling pathways of DCC and INα6β4 in stem cell migration.

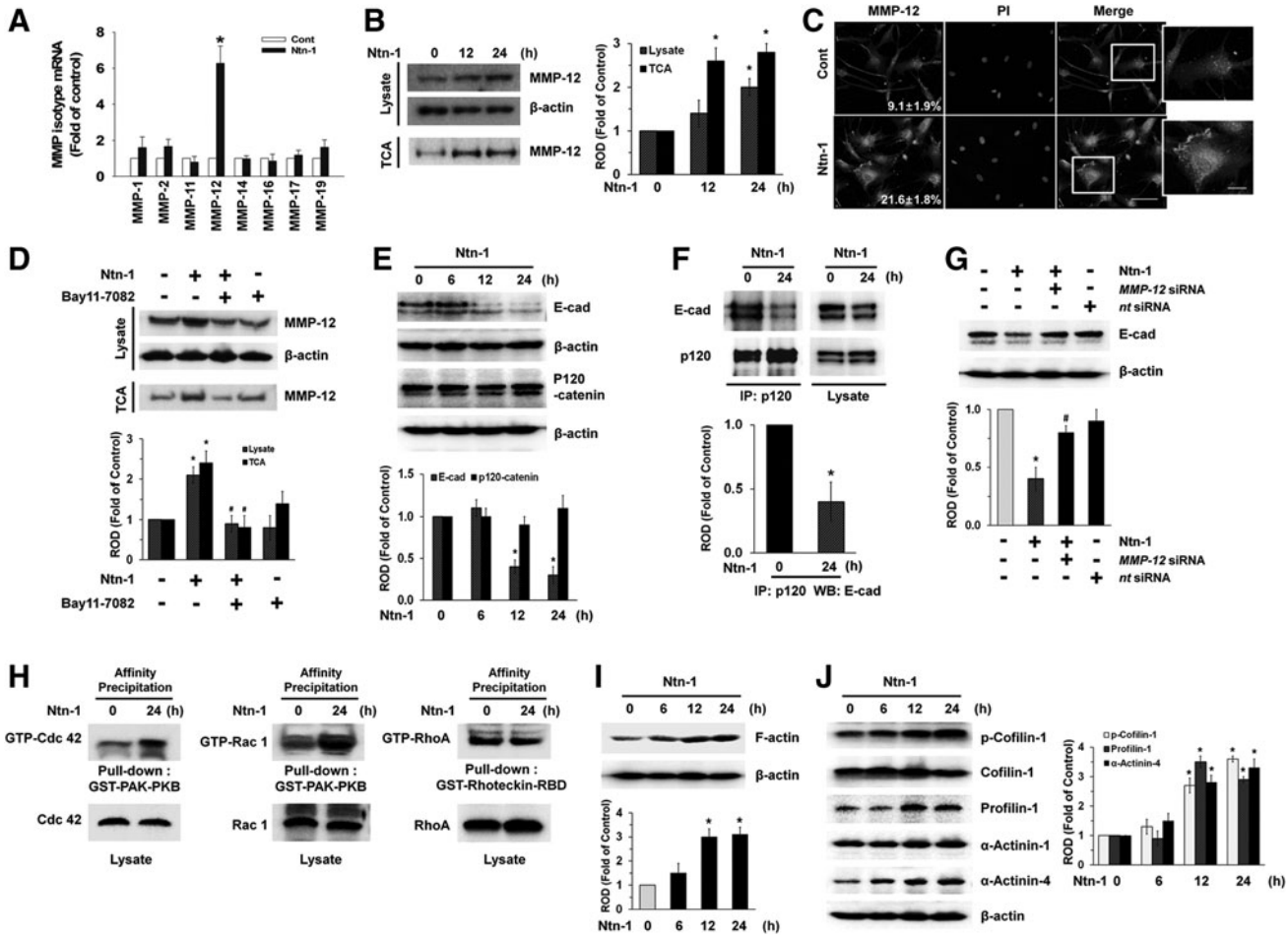

FIG. 4. Effect of Ntn-1 on the degradation of E-cadherin (E-cad) via MMP-12. **(A)** Cells were treated with 50 ng/mL Ntn-1 for 12 h. The mRNA expression of *MMP* family was measured in cells using real-time polymerase chain reaction as described in the Materials and Methods section. Error bars represent the mean ± SE from four independent experiments involving triplicates. $^{*}P < 0.01$ versus control. **(B)** Cells were treated with 50 ng/mL Ntn-1 for 12 or 24 h. Proteins from cell lysates and protein precipitated by TCA in medium were extracted and blotted with MMP-12 antibody. Error bars represent mean ± SE of four independent experiments for each condition determined from densitometry relative to β-actin. $^{*}P < 0.05$ versus 0 h. **(C)** The cells were treated with Ntn-1 (50 ng/mL) for 24 h. MMP-12 was detected by immunostaining with MMP-12 antibody. The expression of MMP-12 was detected by immunostaining with MMP-12 antibody, and quantified by using Image J program. The quantification data of immunofluorescence images were presented as mean ± SE of three independent experiments. Scale bars represent 100 μm (magnification, ×400). PI was used for nuclear counterstaining. **(D)** The cells were pretreated NF-κB inhibitor Bay 11–7082 (10 μM) for 30 min prior to Ntn-1 exposure for 24 h. Proteins from cell lysates and protein precipitated by TCA in medium were extracted and blotted with MMP-12 antibody. Error bars represent mean ± SE of four independent experiments for each condition determined from densitometry relative to β-actin. $^{*}P < 0.01$ versus vehicle. $^{\#}P < 0.01$ versus Ntn-1 alone. **(E)** The cells were incubated in the presence of Ntn-1 (50 ng/mL) for various times (0–24 min) and then harvested. Total protein was extracted and blotted with E-cad and p120-catenin antibodies. Error bars represent the mean ± SE of four independent experiments for each condition determined from densitometry relative to β-actin. $^{*}P < 0.01$ versus 0 h. **(F)** The cells were incubated in the presence of Ntn-1 (50 ng/mL) for 24 h and then harvested. p120-catenin was immunoprecipitated with an anti-p120-catenin antibody, and co-immunoprecipitated E-cad were detected by using anti-E-cad antibody (*left panels*). Expression of p120-catenin and E-cad in total cell lysates is shown in the *right panels*. $n = 4$ Error bars represent the mean ± SE of four independent experiments for each condition determined from densitometry relative p120-catenin binding co-immunoprecipitated with p120-catenin antibody. $^{*}P < 0.01$ versus 0 h. **(G)** Cells were transfected for 24 h with *MMP-12* siRNA (200 pM) using Hyperfectamine before Ntn-1 (50 ng/mL) exposure for 24 h. Nontargeting (*nt*) control siRNA was used as a negative control (200 pM). Total protein was extracted and blotted with E-cad antibody. Error bars represent the mean ± SE of three independent experiments for each condition determined from densitometry relative to β-actin. $^{*}P < 0.01$ versus vehicle. $^{\#}P < 0.05$ versus Ntn-1 alone. **(H)** Cells were treated with Ntn-1 for 24 h, and the lysates (400 μg) were incubated with agarose beads coupled with GST-PAK-PBD or GST-Rhotekin-RBD. The bound activated GTP-Cdc42, GTP-Rac1, and RhoA were resolved by SDS-PAGE, transferred, and blotted using an anti- Cdc42, anti-Rac1, and anti-RhoA antibodies to determine the extent of the activation of Cdc42, Rac1, and RhoA. Total Cdc42, Rac1, and RhoA was determined using lysates (*bottom panels*). Representative results from three independent experiments are shown. **(I, J)** The cells were incubated in the presence of Ntn-1 (50 ng/mL) for various times (0–24 min) and then harvested. Total protein was extracted and blotted with F-actin, phospho-Cofilin-1, Cofilin-1, Profilin-1, α-Actinin-1, and α-Actinin-4 antibodies. Error bars represent mean ± SE of four independent experiments for each condition determined from densitometry relative to β-actin. $^{*}P < 0.01$ versus 0 h. F-actin, filamentous actin; IP, immunoprecipitation; MMP, matrix metalloproteinase; ROD, relative optical density; SDS-PAGE, sodium dodecyl sulfate polyacrylamide gel electrophoresis; TCA, trichloroethanoic acid.

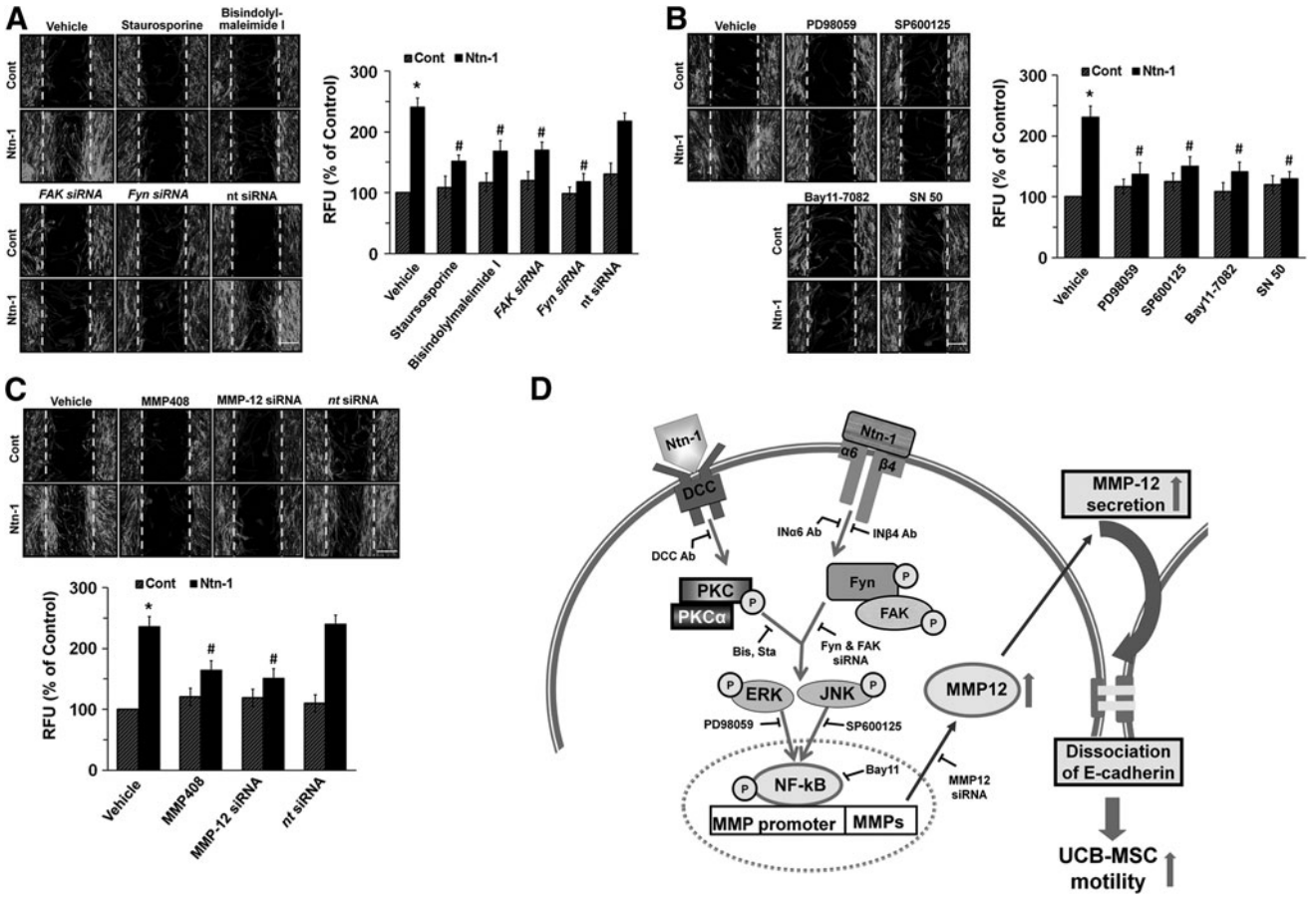

FIG. 5. Role of Ntn-1 and its related signal molecules on human UCB-MSCs motility. **(A)** Cells were pretreated with staurosporine, bisindolylmaleimide I, *FAK siRNA*, *Fyn siRNA*, and *nt siRNA* for 30 min or 24 h prior to Ntn-1 exposure for 24 h. Wound-healing assay (*top panel*) was performed and stained with phalloidin-AlexaFluor 488 to identify the migrating cells. **(B)** Cells were pretreated with PD98059, SP600125, Bay 11-7082, and SN 50 for 30 min prior to Ntn-1 exposure for 24 h and then determined cell motility using wound-healing (*top panel*) and Oris cell migration assays (*bottom panel*). **(C)** Cells were pretreated with MMP408, *MMP-12 siRNA*, and *nt siRNA* for 30 min or 24 h prior to Ntn-1 exposure for 24 h and then determined cell motility using wound-healing (*top panel*) and Oris cell migration assays (*bottom panel*). **(D)** A proposed model for Ntn-1-evoked signaling pathway in promoting motility of human UCB-MSCs. **(A–C)** Error scale bars represent 100 μm (magnification, × 100). Data represent mean ± SE of four independent experiments with triplicate dishes. $^{*}P < 0.01$ versus control. $^{\#}P < 0.05$ versus Ntn-1 alone. MMP, matrix metalloproteinase.

To know that either DCC or INα6β4 has the unique biological properties in relation to Ntn-1-induced cell motility, we first evaluated weather Ntn-1 regulates PKC activation and the release of Ca^{2+} from intracellular stores, which are known to be regulated by DCC during the development of the nervous system [1,24]. Despite its lack of involvement in the influx of calcium, it was found that Ntn-1 induces PKC translocation and phosphorylation, in that PKC is required for DCC activation to promote UCB-MSCs motility. Although the discrepancy with regard to calcium influx may due to differences in species, cell types, or experimental conditions, our results indicate that motility of UCB-MSCs, completely abrogated by the inhibition of PKC pathways, provide strong evidence that PKC plays an important role in the Ntn-1 signaling pathway. These results are consistent with previous study in which galectin-1 increased PKC phosphorylation, but did not affect calcium influx in promoting UCB-MSCs motility [30]. We further found that PKCα, one of several major PKC isoforms, is uniquely activated by Ntn-1. However, it was shown that the activation of PKCα triggers the endocytosis of UNC5, but not DCC, resulting in Ntn-1-mediated axonal responses from repulsion to attraction [31,32]. Since Ntn-1 interaction is limited to DCC or INα6β4 in UCB-MSCs, our results suggest that the effect of Ntn-1 on PKCα activation is likely to be compounded by the selective expression of DCC in UCB-MSCs. On the other hand, we found that Ntn-1 can induce the phosphorylation of FAK/Fyn through INα6β4 and that the silencing of FAK/Fyn inhibits Ntn-1-induced UCB-MSCs migration. FAK is a cytoplasmic protein tyrosine kinase that is involved in multiple cellular processes, including cell migration [33]. Fyn is a Src family kinase related to FAK [8]. Evidence indicates that tyrosine phosphorylation of FAK/Fyn is important for integrin-mediated cell migration [33], suggesting that Ntn-1 coupled with INα6β4 is an important microenvironmental cue in the triggering of FAK/Fyn activation. Thus, these results provide convincing proof that coordination of the Ntn-1/DCC

and Ntn-1/INα6β4 axis is required for human UCB-MSCs motility through the facilitation of the distinct activation of PKCα and Fyn/FAK pathways. Having shown that PKCα and Fyn/FAK are major effector molecules of Ntn-1 signaling pathways in UCB-MSCs, we further attempted to uncover the mechanism how PKCα and Fyn/FAK link to other molecules that are important in the cell migration process. We found that Ntn-1 increases ERK and JNK phosphorylation via the activation of both PKC and Fyn/FAK. This means that DCC/PKCα with INα6β4/FAK/Fyn acts to transduce Ntn-1 signals to ERK/JNK cascades. However, p38 MAPK is not activated by an Ntn-1 treatment, implying a functional role of Ntn-1 in the determination of downstream targets. Moreover, MAPK inhibitors reduce Ntn-1-induced NF-κB phosphorylation and nuclear translocation. Based on these results, we suggest the distinct signaling of DCC and INα6β4 collaborates in the induction of the ERK/JNK/NF-κB pathway to promote UCB-MSCs motility.

To achieve productive forward movement, cell migration must be coupled with destabilizing adherens junctions and extracellular matrix degradation, thereby promoting cell migration [34–36]. MMPs are critical enzymes that digest basement membrane proteins during migration [36,37], but their function in the netrin signaling pathway remain largely unknown. Interestingly, we found that Ntn-1 uniquely increased MMP-12 expression via NF-κB activation in promoting UCB-MSCs motility. Indeed, MMP-12 expression is reportedly essential in tissue remodeling associated with emphysema in mice exposed to cigarette smoke [38]. In addition, MMP-12 null mice have been described as resistant to bleomycin-induced pulmonary fibrosis [39]. Thus, our data provide the first evidence that a MMP-12 is required for the Ntn-1 signaling pathway in promoting UCB-MSCs motility. This change is unique to stem cell migration given that such an effect results from the activation of the intracellular components ERK, JNK, and NF-κB, which are mediated by PKCα and FAK/Fyn in response to Ntn-1. Although the functional role of MMPs in extracellular matrix degradation and remodeling is well established, the effects of MMP on adherens junctions are less well documented. Our results in this study show that Ntn-1 reduces the expression of E-cad via MMP-12 activation. E-cad is the main epithelial cell–cell adhesion molecule, and the downregulation of E-cad-based adherens junctions is a hallmark of cell migration and invasion [26,34,35]. Indeed, MMP-12 has specific elastolytic activity in tissue remodeling [4,38] and can also cleave the extracellular domains of classic cadherin to promote cell proliferation by disrupting cell–cell adhesion [40]. Thus our results indicate that Ntn-1 as a new functional microenvironmental cue promotes the MMP-12-mediated downregulation of E-cad expression during the process of UCB-MSCs motility.

To ensure the importance of E-cad as a relevant mediator of Ntn-1, we further focused on p120-catenin, another critical protein of the adherens junction, which interacts with E-cad to reinforce cell–cell adhesion by forming the cadherin–catenin complex [27,41]. In addition, p120-catenin links cadherins to microtubules and is also important in the prevention of cadherin endocytosis and degradation [42]. In the present study, we found that E-cad coimmunoprecipitates with p120-catenin and, importantly, that the interaction with E-cad is reduced by an Ntn-1 treatment. Thus, Ntn-1 destabilizes cadherin–catenin complex on the plasma membrane accompanied with the downregulation of E-cad expression, thereby allowing cell movement. These results are further supported by previous study in which activated p21-activated kinase enhanced E-cad complex disruption and finally increased the migration of mouse embryonic stem cells [43]. In support of Ntn-1-mediated UCB-MSCs motility, our results further elucidate the potential role of Ntn-1 in the regulation of the cytoskeletal reorganization-related proteins Cdc42, Rac1, Profilin-1, Cofilin-1, α-Actinin-4, and F-actin, which are critical requirements for stem cells migration [44,45]. It is not clear whether this additional effect of Ntn-1 in promoting cytoskeletal reorganization is a sequential result of the loss of cell cohesion or, alternatively, an independent process involving other cellular signaling events. However, it is clearly shown that Profilin-1 and Cofilin-1 play key roles in enhancing the actin assembly at the plasma membrane, thereby increasing F-actin expression that drives cell motility and other actin-linked processes [46,47]. Specifically, α-Actinins cross-links F-actin into bundles to form a cytoskeletal network [48]. Also, recent findings revealed crosstalk between p120-catenin [46] and small Rho GTPases [9]. Thus, it is possible that Ntn-1 stimulates UCB-MSCs motility by regulating MMP-12-dependent E-cad degradation and by governing the cytoskeletal reorganization process.

Collectively, our results suggest that Ntn-1 induces MMP-12-dependent E-cad degradation via the distinct activation of PKCα and FAK/Fyn in promoting motility of MSCs (Fig. 5D). Thus, highlighting signaling pathways involved in Ntn-1-stimulated motility of UCB-MSCs may provide potential targets for strategic modulation of stem cell transplantation. In conclusion, Ntn-1 requires the DCC/PKCα and INα6β/FAK/Fyn pathways, with both being necessary for ERK/JNK/NF-κB activation. It thereby controls the MMP-mediated E-cad downregulation and E-cad-p120-catenin interaction in promoting motility of UCB-MSCs.

Acknowledgments

This study was supported by a grant of the Korean Health Technology R&D Project, Ministry of Health and Welfare, Republic of Korea (A120216), and a grant from the Next-Generation BioGreen 21 Program (no. PJ009090), Rural Development Administration, Republic of Korea.

Author Disclosure Statement

The authors declare no conflict of interest.

References

1. Lai Wing Sun K, JP Correia and TE Kennedy. (2011). Netrins: versatile extracellular cues with diverse functions. Development 138:2153–2169.
2. Bongo JB and DQ Peng. (2014). The neuroimmune guidance cue netrin-1: a new therapeutic target in cardiovascular disease. J Cardiol 63:95–98.
3. Barallobre MJ, M Pascual, JA Del Rio and E Soriano. (2005). The Netrin family of guidance factors: emphasis on Netrin-1 signalling. Brain Res Brain Res Rev 49:22–47.

4. Cirulli V and M Yebra. (2007). Netrins: beyond the brain. Nat Rev Mol Cell Biol 8:296–306.
5. Son TW, SP Yun, MS Yong, BN Seo, JM Ryu, HY Youn, YM Oh and HJ Han. (2013). Netrin-1 protects hypoxia-induced mitochondrial apoptosis through HSP27 expression via DCC- and integrin α6β4-dependent Akt, GSK-3β, and HSF-1 in mesenchymal stem cells. Cell Death Dis 4:e563.
6. Yebra M, AM Montgomery, GR Diaferia, T Kaido, S Silletti, B Perez, ML Just, S Hildbrand, R Hurford, et al. (2003). Recognition of the neural chemoattractant Netrin-1 by integrins α6β1 and α3β1 regulates epithelial cell adhesion and migration. Dev Cell 5:695–707.
7. Liu G, H Beggs, C Jurgensen, HT Park, H Tang, J Gorski, KR Jones, LF Reichardt, J Wu and Y Rao. (2004). Netrin requires focal adhesion kinase and Src family kinases for axon outgrowth and attraction. Nat Neurosci 7:1222–1232.
8. Thomas SM and JS Brugge. (1997). Cellular functions regulated by Src family kinases. Annu Rev Cell Dev Biol 13:513–609.
9. Shekarabi M and TE Kennedy. (2002). The netrin-1 receptor DCC promotes filopodia formation and cell spreading by activating Cdc42 and Rac1. Mol Cell Neurosci 19:1–17.
10. Forcet C, E Stein, L Pays, V Corset, F Llambi, M Tessier-Lavigne and P Mehlen. (2002). Netrin-1-mediated axon outgrowth requires deleted in colorectal cancer-dependent MAPK activation. Nature 417:443–447.
11. Yang SE, CW Ha, M Jung, HJ Jin, M Lee, H Song, S Choi, W Oh and YS Yang. (2004). Mesenchymal stem/progenitor cells developed in cultures from UC blood. Cytotherapy 6:476–486.
12. Qiao C, W Xu, W Zhu, J Hu, H Qian, Q Yin, R Jiang, Y Yan, F Mao, et al. (2008). Human mesenchymal stem cells isolated from the umbilical cord. Cell Biol Int 32:8–15.
13. Le Blanc K, L Tammik, B Sundberg, SE Haynesworth and O Ringden. (2003). Mesenchymal stem cells inhibit and stimulate mixed lymphocyte cultures and mitogenic responses independently of the major histocompatibility complex. Scand J Immunol 57:11–20.
14. Jeong JA, SH Hong, EJ Gang, C Ahn, SH Hwang, IH Yang, H Han and H Kim. (2005). Differential gene expression profiling of human umbilical cord blood-derived mesenchymal stem cells by DNA microarray. Stem Cells 23:584–593.
15. Sensebe L, M Krampera, H Schrezenmeier, P Bourin and R Giordano. (2010). Mesenchymal stem cells for clinical application. Vox Sang 98:93–107.
16. Wakitani S, M Nawata, K Tensho, T Okabe, H Machida and H Ohgushi. (2007). Repair of articular cartilage defects in the patello-femoral joint with autologous bone marrow mesenchymal cell transplantation: three case reports involving nine defects in five knees. J Tissue Eng Regen Med 1:74–79.
17. Peled A, I Petit, O Kollet, M Magid, T Ponomaryov, T Byk, A Nagler, H Ben-Hur, A Many, et al. (1999). Dependence of human stem cell engraftment and repopulation of NOD/SCID mice on CXCR4. Science 283:845–848.
18. Son BR, LA Marquez-Curtis, M Kucia, M Wysoczynski, AR Turner, J Ratajczak, MZ Ratajczak and A Janowska-Wieczorek. (2006). Migration of bone marrow and cord blood mesenchymal stem cells in vitro is regulated by stromal-derived factor-1-CXCR4 and hepatocyte growth factor-c-met axes and involves matrix metalloproteinases. Stem Cells 24:1254–1264.
19. Lee MJ, ES Jeon, JS Lee, M Cho, DS Suh, CL Chang and JH Kim. (2008). Lysophosphatidic acid in malignant ascites stimulates migration of human mesenchymal stem cells. J Cell Biochem 104:499–510.
20. Fu X, B Han, S Cai, Y Lei, T Sun and Z Sheng. (2009). Migration of bone marrow-derived mesenchymal stem cells induced by tumor necrosis factor-α and its possible role in wound healing. Wound Repair Regen 17:185–191.
21. Chieng-Yane P, A Bocquet, R Letienne, T Bourbon, S Sablayrolles, M Perez, SN Hatem, AM Lompre, B Le Grand and M David-Dufilho. (2011). Protease-activated receptor-1 antagonist F 16618 reduces arterial restenosis by down-regulation of tumor necrosis factor α and matrix metalloproteinase 7 expression, migration, and proliferation of vascular smooth muscle cells. J Pharmacol Exp Ther 336:643–651.
22. Park JH and HJ Han. (2009). Caveolin-1 plays important role in EGF-induced migration and proliferation of mouse embryonic stem cells: involvement of PI3K/Akt and ERK. Am J Physiol Cell Physiol 297:C935–C944.
23. Bradford MM. (1976). A rapid and sensitive method for the quantitation of microgram quantities of protein utilizing the principle of protein-dye binding. Anal Biochem 72:248–254.
24. Xie Y, Y Hong, XY Ma, XR Ren, S Ackerman, L Mei and WC Xiong. (2006). DCC-dependent phospholipase C signaling in netrin-1-induced neurite elongation. J Biol Chem 281:2605–2611.
25. Paradisi A and P Mehlen. (2010). Netrin-1, a missing link between chronic inflammation and tumor progression. Cell Cycle 9:1253–1262.
26. Berx G and F Van Roy. (2001). The E-cadherin/catenin complex: an important gatekeeper in breast cancer tumorigenesis and malignant progression. Breast Cancer Res 3:289–293.
27. Kourtidis A, SP Ngok and PZ Anastasiadis. (2013). p120 catenin: an essential regulator of cadherin stability, adhesion-induced signaling, and cancer progression. Prog Mol Biol Transl Sci 116:409–432.
28. Li Q, D Yao, J Ma, J Zhu, X Xu, Y Ren, X Ding and X Mao. (2011). Transplantation of MSCs in combination with netrin-1 improves neoangiogenesis in a rat model of hind limb ischemia. J Surg Res 166:162–169.
29. Petrie RJ, AD Doyle and KM Yamada. (2009). Random versus directionally persistent cell migration. Nat Rev Mol Cell Biol 10:538–549.
30. Yun SP, SJ Lee, YH Jung and HJ Han. (2014). Galectin-1 stimulates motility of human umbilical cord blood-derived mesenchymal stem cells by downregulation of smad2/3-dependent collagen 3/5 and upregulation of NF-κB-dependent fibronectin/laminin 5 expression. Cell Death Dis 5:e1049.
31. Williams ME, SC Wu, WL McKenna and L Hinck. (2003). Surface expression of the netrin receptor UNC5H1 is regulated through a protein kinase C-interacting protein/protein kinase-dependent mechanism. J Neurosci 23:11279–11288.
32. Bartoe JL, WL McKenna, TK Quan, BK Stafford, JA Moore, J Xia, K Takamiya, RL Huganir and L Hinck. (2006). Protein interacting with C-kinase 1/protein kinase Cα-mediated endocytosis converts netrin-1-mediated repulsion to attraction. J Neurosci 26:3192–3205.
33. Mierke CT. (2013). The role of focal adhesion kinase in the regulation of cellular mechanical properties. Phys Biol 10:065005.
34. McGuire JK, Q Li and WC Parks. (2003). Matrilysin (matrix metalloproteinase-7) mediates E-cadherin ectodomain

shedding in injured lung epithelium. Am J Pathol 162: 1831–1843.
35. Cowden Dahl KD, J Symowicz, Y Ning, E Gutierrez, DA Fishman, BP Adley, MS Stack and LG Hudson. (2008). Matrix metalloproteinase 9 is a mediator of epidermal growth factor-dependent e-cadherin loss in ovarian carcinoma cells. Cancer Res 68:4606–4613.
36. Bourboulia D, H Han, S Jensen-Taubman, N Gavil, B Isaac, B Wei, L Neckers and WG Stetler-Stevenson. (2013). TIMP-2 modulates cancer cell transcriptional profile and enhances E-cadherin/β-catenin complex expression in A549 lung cancer cells. Oncotarget 4:163–173.
37. Kang H, M Lee, KC Choi, DM Shin, J Ko and SW Jang. (2012). N-(4-hydroxyphenyl)retinamide inhibits breast cancer cell invasion through suppressing NF-κB activation and inhibiting matrix metalloproteinase-9 expression. J Cell Biochem 113:2845–2855.
38. Hautamaki RD, DK Kobayashi, RM Senior and SD Shapiro. (1997). Requirement for macrophage elastase for cigarette smoke-induced emphysema in mice. Science 277:2002–2004.
39. Dunsmore SE, J Roes, FJ Chua, AW Segal, SE Mutsaers and GJ Laurent. (2001). Evidence that neutrophil elastase-deficient mice are resistant to bleomycin-induced fibrosis. Chest 120:35S–36S.
40. Dwivedi A, SC Slater and SJ George. (2009). MMP-9 and -12 cause N-cadherin shedding and thereby β-catenin signalling and vascular smooth muscle cell proliferation. Cardiovasc Res 81:178–186.
41. Yanagisawa M and PZ Anastasiadis. (2006). p120 catenin is essential for mesenchymal cadherin-mediated regulation of cell motility and invasiveness. J Cell Biol 174:1087–1096.
42. Bartlett JD and CE Smith. (2013). Modulation of cell-cell junctional complexes by matrix metalloproteinases. J Dent Res 92:10–17.
43. Suh HN and HJ Han. (2010). Laminin regulates mouse embryonic stem cell migration: involvement of Epac1/Rap1 and Rac1/cdc42. Am J Physiol Cell Physiol 298: C1159–C1169.
44. Park SS, MO Kim, SP Yun, JM Ryu, JH Park, BN Seo, JH Jeon and HJ Han. (2013). C(16)-Ceramide-induced F-actin regulation stimulates mouse embryonic stem cell migration: involvement of N-WASP/Cdc42/Arp2/3 complex and cofilin-1/α-actinin. Biochim Biophys Acta 1831:350–360.
45. Yun SP, JM Ryu, MO Kim, JH Park and HJ Han. (2012). Rapid actions of plasma membrane estrogen receptors regulate motility of mouse embryonic stem cells through a profilin-1/cofilin-1-directed kinase signaling pathway. Mol Endocrinol 26:1291–1303.
46. Menke A and K Giehl. (2012). Regulation of adherens junctions by Rho GTPases and p120-catenin. Arch Biochem Biophys 524:48–55.
47. Konakahara S, K Ohashi, K Mizuno, K Itoh and T Tsuji. (2004). CD29 integrin- and LIMK1/cofilin-mediated actin reorganization regulates the migration of haematopoietic progenitor cells underneath bone marrow stromal cells. Genes Cells 9:345–358.
48. Araki N, T Hatae, T Yamada and S Hirohashi. (2000). Actinin-4 is preferentially involved in circular ruffling and macropinocytosis in mouse macrophages: analysis by fluorescence ratio imaging. J Cell Sci 113 (Pt 18):3329–3340.

Address correspondence to:
Dr. Ho Jae Han
Department of Veterinary Physiology
College of Veterinary Medicine
Seoul National University
Gwanak-ro
Gwanak-gu
Seoul 151-742
South Korea

E-mail: hjhan@snu.ac.kr

Received for publication December 22, 2013
Accepted after revision March 27, 2014
Prepublished on Liebert Instant Online April 16, 2014